Nanometer-Thick Surficial Films in Oxides as a Case of Prewetting

Jian Luo

School of Materials Science and Engineering and Center for Optical Materials Science and Engineering Technologies, Clemson University, Clemson, South Carolina

Yet-Ming Chiang*

Department of Materials Science and Engineering, Massachusetts Institute of Technology, Cambridge, Massachusetts 02139

Rowland M. Cannon

Lawrence Berkeley National Laboratory, University of California, Berkeley, California

Received February 28, 2005. In Final Form: May 4, 2005

Stable, nanometer-thick films are observed to form at the $\{11\bar{2}0\}$ facets of Bi_2O_3-doped ZnO in several bulk-phase stability fields. Electron microscopy shows these surficial films to exhibit some degree of partial order in quenched samples. The equilibrium film thickness, corresponding to the Gibbs excess solute, decreases monotonically with decreasing temperature until vanishing at a dewetting temperature, well below the eutectic. Assuming that perfect wetting occurs at some higher temperature above the eutectic, as is observed on polycrystal surfaces and at grain boundaries in the same system, the adsorption and wetting events in this system illustrate temperature- and composition-dependent prewetting. The observation of a second class of thicker films coexisting with nanodroplets and a numerical evaluation of thickness versus temperature elucidate the critical role of volumetric thermodynamic terms in determining film stability and thickness. Analogous temperature-dependent surface films involving adsorbed MoO_3 on Al_2O_3 were also observed.

1. Introduction

Nanometer-thick, disordered films of a nearly constant or "equilibrium" thickness (often termed intergranular films, IGFs) have been widely observed at grain boundaries in ceramic systems.[1−15] These can alternatively be understood to be multilayer adsorbates with compositions set by the chemical potentials of the bulk phases[13,14] or liquidlike layers that adopt a constant thickness in response to a balance among several specific interactions that individually may act to thin or thicken the film.[1,4,10,12−14] Among oxides, a considerable body of data has accumulated for the ZnO−Bi_2O_3 system,[8−10,15] which is the prototypical varistor and an exemplar of activated sintering.[15] Figure 1a shows an example of an IGF in ZnO doped with Bi_2O_3 that is characteristic of high-angle grain boundaries.[8−10] Recently, a free surface counterpart of the equilibrium-thickness intergranular films has been found[15−18] (Figure 1b); these are termed surficial amorphous films, SAFs, despite indications of some local order within them.

Disordered surficial films of this type have been observed in several two-component oxide systems, of which ZnO−Bi_2O_3 has been most extensively studied.[16−18] These films have several unique characteristics. Although no film has been observed to form on surfaces of $\{1\bar{1}00\}$ orientation, facets with associated films are almost always observed at the $\{11\bar{2}0\}$ surface. Because Bi_2O_3 is also found to crystallize heteroepitaxially at this same surface,[17] the anisotropy has been attributed to induced order between this ZnO surface and bismuth oxide structural units constituting the film, which may lower the crystal−film interfacial energy and stabilize the surficial film. In samples saturated with Bi_2O_3, these films take on a nearly constant thickness at a fixed firing temperature. Once an equilibrium state has been reached, variations in additional firing time and the amount of bulk, extra secondary phases have no discernible influence on the average value of, or variability in, film thickness. Like

(1) Clarke, D. R. *J. Am. Ceram. Soc.* **1987**, *70*, 15−22.
(2) Kleebe, H.-J.; Hoffman, M. J.; Rühle, M. *Z. Metallkd.* **1992**, *83*, 610−617.
(3) Kleebe, H.-J.; Cinibulk, M. K.; Cannon, R. M.; Rühle, M. *J. Am. Ceram. Soc.* **1993**, *76*, 1969−1977.
(4) Clarke, D. R.; Shaw, T. M.; Philipse, A. P.; Horn, R. G. *J. Am. Ceram. Soc.* **1993**, *76*, 1201−1204.
(5) Tanaka, I.; Kleebe, H.-J.; Cinibulk, M. K.; Bruley, J.; Clarke, D. R.; Rühle, M. *J. Am. Ceram. Soc.* **1994**, *77*, 911−914.
(6) Chiang, Y.-M.; Silverman, L. A.; French, R. H.; Cannon, R. M. *J. Am. Ceram. Soc.* **1994**, *77*, 143−152.
(7) Ackler, H. D.; Chiang, Y.-M. *J. Am. Ceram. Soc.* **1997**, *80*, 1893−1896.
(8) Lee, J.-R.; Chiang, Y.-M.; Ceder, G. *Acta Metall. Mater.* **1997**, *45*, 1247−1257.
(9) Wang, H.; Chiang, Y.-M. *J. Am. Ceram. Soc.* **1998**, *81*, 89−96.
(10) Chiang, Y.-M.; Wang, H.; Lee, J.-R. *J. Microsc.* **1998**, *191*, 275−285.
(11) Ackler, H. D.; Chiang, Y.-M. *J. Am. Ceram. Soc.* **1999**, *82*, 183−189.
(12) Bobeth, M.; Clarke, D. R.; Pompe, W. *J. Am. Ceram. Soc.* **1999**, *82*, 1537−1546.
(13) Cannon, R. M.; Esposito, L. *Z. Metallkd.* **1999**, *90*, 1002−1015.
(14) Cannon, R. M.; Rühle, M.; Hoffmann, M. J.; French, R. H.; Gu, H.; Tomsia, A. P.; Saiz, E. In *Ceramic Transactions*; Sakuma, T., Ikuhara, Y., Eds.; The American Ceramic Society: Westerville, OH, 2000; Vol. 12, pp 427−444.
(15) Luo, J.; Wang, H.; Chiang, Y.-M. *J. Am. Ceram. Soc.* **1999**, *82*, 916−920.
(16) Luo, J.; Chiang, Y.-M. *J. Eur. Ceram. Soc.* **1999**, *19*, 697−701.
(17) Luo, J.; Chiang, Y.-M. *Acta Mater.* **2000**, *48*, 4501−4515.
(18) Luo, J. Existence and Stability of Nanometer-Thick Disordered Films on Oxide Surfaces. Ph.D. Thesis, Massachusetts Institute of Technology, Cambridge, MA, 2001.

10.1021/la0505420 CCC: $30.25
Published on Web 07/02/2005

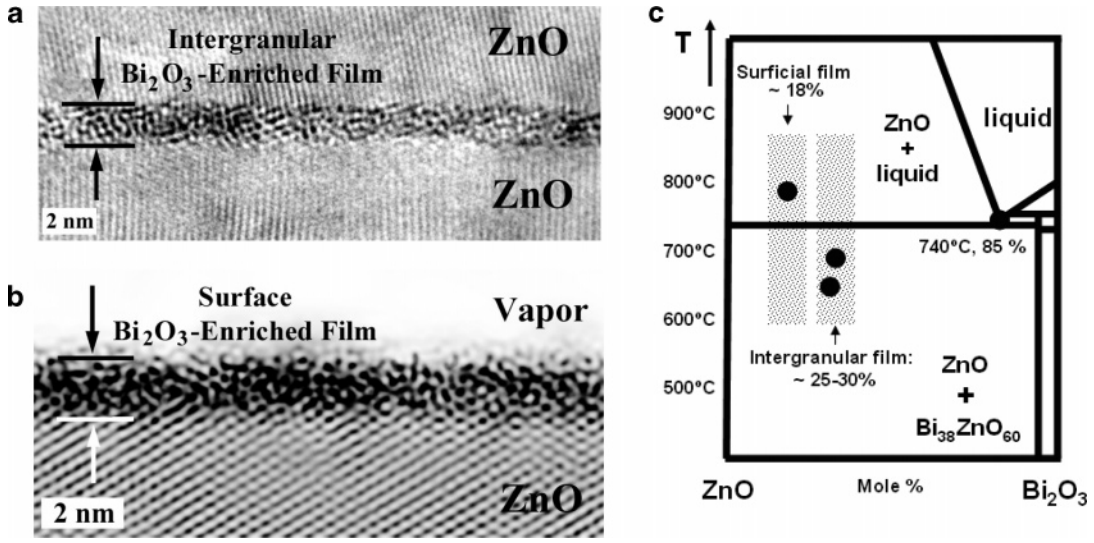

Figure 1. (a) Equilibrium thickness intergranular film, IGF, that is characteristic of high-angle grain boundaries in Bi_2O_3-doped ZnO.[8−10,15] (b) Free surface counterpart,[15−18] (i.e., a Bi_2O_3-enriched surficial amorphous film, SAF, on the ZnO $\{11\bar{2}0\}$ facets). (c) Distinct film compositions schematically illustrated in the phase fields of the binary phase diagram. The solid dots represent actual composition measurements for films coexisting with Bi-rich second phases.[9,10,17]

IGFs in ZnO−Bi_2O_3,[9,10] the surficial thin films are markedly different in composition from bulk liquids that are stable at the experimental temperature. The average measured molar percentage of Bi_2O_3 in the film is 18 mol %,[17] being distinctly Zn-rich compared to the near-eutectic equilibrium bulk liquid (~83 mol % Bi_2O_3)[19] (Figure 1c). Films with the same characteristics are observed in several phase fields, namely, in Bi_2O_3-saturated samples equilibrated slightly above the bulk eutectic temperature, where they coexist with ZnO and a nonwetting bulk liquid phase, below the eutectic temperature, where they coexist with two crystalline bulk phases, and in single-phase ZnO solid solutions containing a smaller amount of Bi_2O_3, where they are somewhat thinner.

The stabilization of a thin surficial layer enriched in a surface-active element has a clear parallel to Cahn's prewetting and critical-point wetting model[20−26] that was initially proposed for surface adsorption in fluid systems, wherein a balance between reduction in the "short-range" surface-energy term and the increase in the excess free energy integral over the film volume (in the phase-field formula shown as eq 4 in reference 20) can stabilize a film with a nonzero, finite thickness. If this is true, then monotonically decreasing film thickness with decreasing temperature and dopant chemical potential in subeutectic and subsolidus regimes, as well as complete dewetting and drying of films at lower temperatures, can be expected, in contrast to conventional Langmuir−McLean adsorption, which more often tends to diminish with heating. Unlike Cahn's original prewetting model that was proposed for fluid systems, both structural (i.e., disordering/amorphization) and compositional contributions to the free-energy terms are important to understand the formation of disordered films on crystalline surfaces. The stabilization of disordered films below the relevant eutectic temperatures is also analogous to the formation of premelted surface layers on ice and other one-component systems below the bulk melting points.[27,28]

In systems having an attractive London dispersion interaction, the finite surficial films should persist into the solid−liquid coexistence regime with gradual thickening upon heating. Analogous to Cahn's prewetting and critical-point wetting model, perfect wetting may also be expected to exist at some higher temperatures. By mapping the appearance and disappearance of films and the temperature-dependent equilibrium thicknesses, an interpretation of these phenomena in terms of prewetting and perfect wetting becomes possible, but Cahn's original model must be further modified to consider these more complex binary eutectic systems. The purpose of the present study is to explore and test the above concepts.

2. Experimental Procedure

Homogeneous Bi_2O_3-doped ZnO oxide powders (~100 nm) were synthesized by a solution-chemical process.[8] MoO_3-doped Al_2O_3 samples were produced by annealing a mixture of ultrafine alumina powders and the MoO_3 additive. The doped powders were fired at elevated temperatures in closed containers to achieve thermal equilibrium and were air quenched. A mixture of bulk ZnO and Bi_2O_3 powder was used as a buffer to keep constant vapor pressures for saturated samples that were annealed for 24 h or longer. Transmission electron microscopy (TEM) specimens were prepared by dispersing the powders ultrasonically in acetone and dropping a small amount of the suspension onto carbon-coated copper grids. The powder surfaces were characterized by high-resolution transmission electron microscopy (HRTEM) using a JEM 2010 (JEOL Ltd., Tokyo, Japan) microscope equipped with an energy-dispersive X-ray (EDX) analyzer.

3. Results

3.1. Bi_2O_3 on ZnO: Film Characteristics. Bi_2O_3-enriched disordered films have been observed to form on more than 200 ZnO particle surfaces of $\{11\bar{2}0\}$ orientation.

(19) Safronov, G. M.; Batog, V. N.; Stepanyuk, T. V.; Fedorov, P. M. *Russ. J. Inorg. Chem.* **1971**, *16*, 460−461.
(20) Cahn, J. W. *J. Chem. Phys.* **1977**, *66*, 3667−3672.
(21) Sullivan, D. E.; Telo da Gama, M. M. In *Fluid Interfacial Phenomena*; Croxton, C. A., Ed.; John Wiley and Sons: New York, 1986; pp 45−134.
(22) Dietrich, S. In *Phase Transitions in Surface Films*; Taub, H. E. A., Ed.; Plenum Press: New York, 1991; pp 391−423.
(23) Schmidt, J. W.; Moldover, M. R. *J. Chem. Phys.* **1986**, *84*, 4563.
(24) Wynblatt, P.; Chatain, D. *Ber Bunsen-Ges. Phys. Chem.* **1998**, *102*, 1142−1150.
(25) Kellay, H.; Bonn, D.; Meunier, J. *Phys. Rev. Lett.* **1993**, *71*, 2607−2610.
(26) Lucht, B.; Bahr, C. *Phys. Rev. Lett.* **1998**, *80*, 3783−3786.
(27) Dash, J. G. *Contemp. Phys.* **1989**, *30*, 89−100.
(28) Dash, J. G.; Fu, H.; Wettlaufer, J. S. *Rep. Prog. Phys.* **1995**, *58*, 115−167.

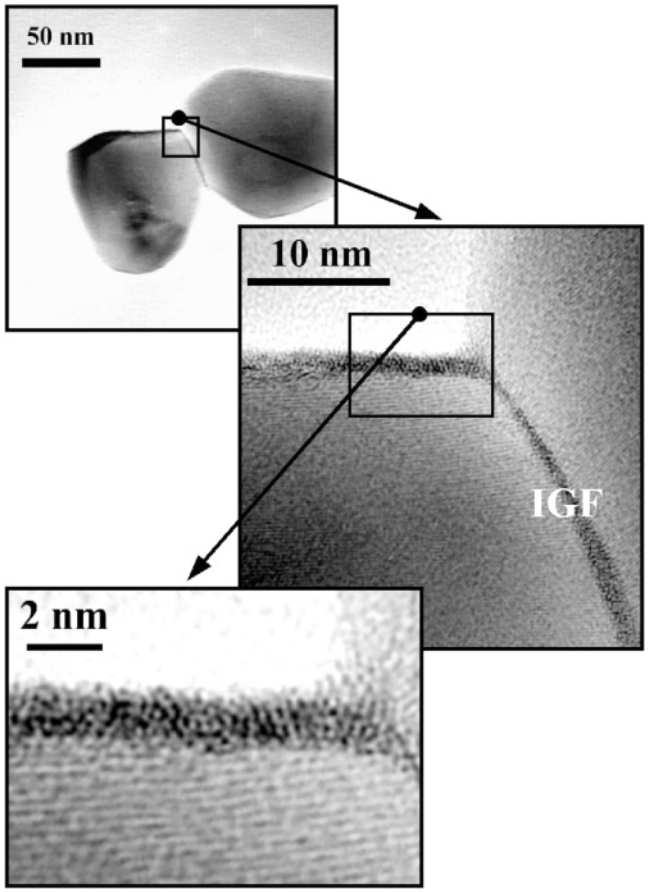

Figure 2. Representative TEM images of a particle surface. A disordered SAF is seen. An IGF of the same character is also labeled. The sample contains 0.58 mol % Bi_2O_3 and has been annealed at 600 °C for 96 h.

A set of representative TEM images of a particle surface, from low to high magnifications, is shown in Figure 2. Some surface films appear to be largely disordered in HRTEM images (Figures 1b and 2), whereas others exhibit some degree of order. A layering structure (Figure 3a) was frequently observed in samples equilibrated both above and below the bulk eutectic temperature. The interlayer distance in the adsorbates is typically slightly greater than that in the bulk; digital image processing of Figure 3a showed that the distance between the first and second adsorbed layers is ~0.40 nm and the ZnO $\{11\bar{2}0\}$ lattice spacing is 0.325 nm. Occasionally, we observed lateral ordering (Figure 3b) whose period is double the ZnO $\{1\bar{1}00\}$ lattice spacing. In Figure 3b, the sample is aligned to show the parallel ZnO $\{1\bar{1}00\}$ lattice fringes and slightly tilted around the perpendicular $\langle 11\bar{2}0\rangle$ axis to show the lateral ordering clearly. It is, therefore, unclear whether the observed lateral order is largely localized at the film−crystal transition or exists throughout the film. Although most surficial films exhibit some degree of partial or local order, it is important to note that all observation are made for quenched samples and the two images shown in Figure 3 represent the most ordered, rather than the typical, observed films.

3.2. Bi_2O_3 on ZnO: Temperature Dependence of Film Thickness. To probe the film temperature dependence and to identify any kinetic limitations to equilibration, the surficial films in a saturated sample were allowed to approach their equilibrium state from both lower and higher temperatures. In the first instance, samples were directly heated to a particular annealing temperature and equilibrated. In the second, samples were first fired at a higher temperature of 780 °C, at which thicker films are known to form, and then the temperature was lowered to the equilibration temperature. Figure 4 shows a reversible temperature dependence on film thickness for saturated samples, decreasing with decreasing temperature.

As the equilibration temperature is lowered to 600 °C, we begin to see kinetic limitations to equilibration in the experiment. When the saturated sample was equilibrated after having first been fired at 780 °C, films were observed on virtually all $\{11\bar{2}0\}$ facets. However, when the same starting powder was heated from room temperature, SAFs were identified to form only on approximately two-thirds of the surfaces in the vicinity of the $\{11\bar{2}0\}$ orientation. (Most of the surfaces without SAFs are not faceted.) In Figure 4, the average film thickness for this sample represents only the 17 surfaces where films were observed, and 9 surfaces without films are excluded. Films were observed on virtually all $\{11\bar{2}0\}$ facets in samples equilibrated at 650 °C and higher temperatures.

To seek the complete drying (dewetting) of surface films, a low-temperature prolonged annealing experiment was conducted. A saturated sample was first fired at 780 °C, at which equilibrium surface films are known to form, and then annealed at 450 °C for 6 months (4392 h). An examination of over 100 particles revealed the disappearance of uniform SAFs in the thickness range originally observed. In general, $\{11\bar{2}0\}$ facets that had been stabilized by forming SAFs at 780 °C disappeared at 450 °C. In a few cases, $\{11\bar{2}0\}$ facets devoid of distinguishable films were observed (Figure 5).

3.3. Bi_2O_3 on ZnO: Films in Local Equilibrium with Nanodroplets. A second class of thicker films coexisting with nanodroplets (5−15 nm) of bismuth-rich oxide liquid or glass (Figure 6, Table 1) has also been observed in this study. This class of films was observed in the same set of samples but on a small fraction of particle surfaces. These may exist where a larger initial surface excess has not been completely evaporated during annealing or possibly formed by condensation during cooling. Consistently, the coexisting films are found to be thicker. These thicker SAFs can be interpreted as a metastable equilibration in a closed system where the total surface excess is restricted by the relatively slow evaporation kinetics (needed to move excess Bi_2O_3 to the second-phase regions), but the amorphous phase can still redistribute locally through surface diffusion to lower the free energy (as opposed to the true equilibrium films in an open system where the chemical potential is specified by large-sized bulk phases).

In saturated samples equilibrated at 780 and 700 °C, the mean thicknesses of SAFs in equilibrium with nanodroplets are 1.85 and 1.90 nm, respectively. These films are 0.3−0.6 nm thicker than those in true equilibrium (i.e., without the presence of nanodroplets), and these differences are one to two standard deviations of the thickness distributions (Table 1). A statistical *t* test[29] has been conducted to verify that these are not random errors or extremes within the same population. The >99% levels of significance imply that the differences between the two groups very likely are real.

3.4. MoO_3 on Al_2O_3. In ZnO−Bi_2O_3, we have studied one crystalline orientation of one system carefully and have found a narrow distribution of temperature-dependent film thicknesses. Films containing MoO_3 on Al_2O_3 represent a second system where similar trends in surface adsorption have been identified, although the majority of

(29) Rade, L.; Westergren, B. In *Mathematics Handbook for Science and Engineering*, 4th ed.; Springer: New York, 1999.

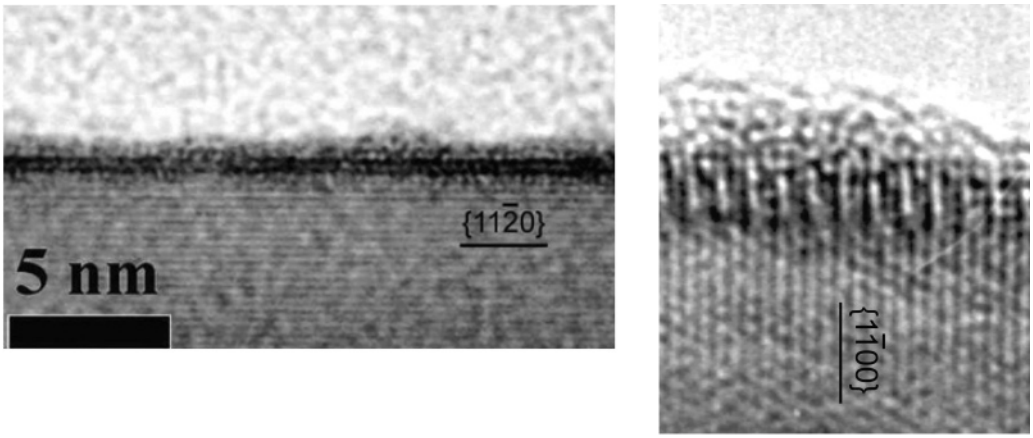

Figure 3. Partial order observed in many quenched films, including (a) the layering structure and (b) the lateral order whose period doubles the ZnO {1$\bar{1}$00} lattice distance. In b, the sample is aligned to show the parallel ZnO {1$\bar{1}$00} lattice fringes and is slightly tilted around the perpendicular ⟨11$\bar{2}$0⟩ axis to show the lateral ordering clearly. Both samples contain 0.58 mol % Bi_2O_3 and have been equilibrated at 780 °C.

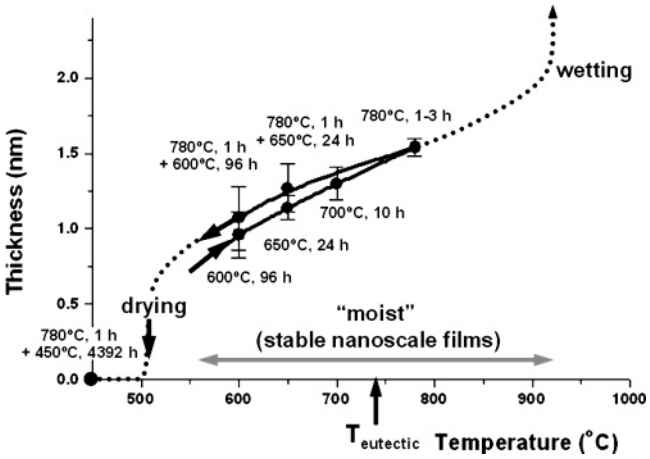

Figure 4. Average thickness vs temperature for Bi_2O_3-enriched films formed on the ZnO {11$\bar{2}$0} facet in saturated samples. The equilibration times and heat treatment histories are labeled. Bars represent 95% confidence intervals.

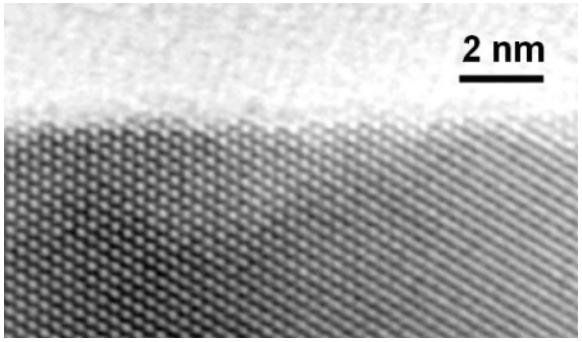

Figure 5. Dried {11$\bar{2}$0} facet equilibrated at 450 °C. The sample, containing 0.58 mol % Bi_2O_3, has been annealed at 780 °C for 1 h, at which equilibrium SAFs are known to form, and then annealed at 450 °C for 6 months.

the adsorbates formed at higher temperature appear as ordered bilayers (Figure 7b) instead of disordered films (Figure 7c). Nanometer-sized γ-Al_2O_3 powder was mixed with MoO_3 powder (1 g of Al_2O_3/0.1 g of MoO_3) and annealed at elevated temperature. After firing at temperatures of 450−650 °C, no distinguishable films were observed (Figure 7a). Some surface segregation of molybdenum, although it cannot be seen in Figure 7a, was confirmed

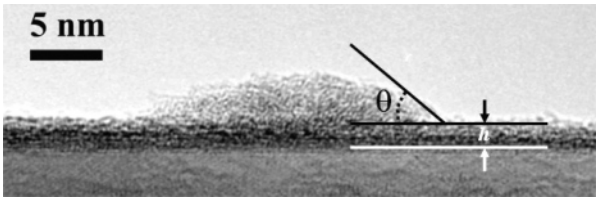

Figure 6. Surficial film coexisting with a nonwetting nanodroplet. The sample contains 0.58 mol % Bi_2O_3 and has been annealed at 700 °C for 10 h. This SAF is 1.95 nm thick, whereas the average thickness for films without the presence of nanodroplets is 1.30 nm.

by X-ray compositional analysis by focusing the e-beam (∼5 nm diameter) on the surface. After higher firing temperatures (900−975 °C, $T_{melting}$ = 795 °C for MoO_3), a unique bilayer adsorbate of ∼0.7 nm thickness, which corresponds to a double octahedral layer of the α-MoO_3 structure[30] as shown in the inset of Figure 7b, was observed on a large portion of the surfaces (Figure 7c), whereas many other facets remained dry. In a few instances (<5% of all Al_2O_3 surfaces), 1−2-nm-thick surface amorphous films were also observed (Figure 7c), but the conditions for forming these thicker disordered surficial films are unclear; for a subset of these, a nanodroplet of Mo-rich amorphous material was also present nearby. A limited number of electron diffraction patterns did not provide a conclusive identification of phase and orientation.

4. Discussion

The surficial films reported in this and earlier papers[16,17] appear to share similar characteristics with equilibrium-thickness intergranular films in ceramics.[1−5] In ZnO−Bi_2O_3, these films have been more extensively characterized; both the surficial and intergranular films[8−10] exhibit

(1) some degree of partial order in quenched samples;

(2) an equilibrium thickness that exhibits a clear dependence on firing temperature and adsorbate/solute chemical potential over a significant temperature range;

(3) similar character in multiphase samples equilibrated above and below the bulk eutectic temperature, 740 °C, and in single-phase samples within the solid solubility limit; and

(30) Smith, R. L. The Structural Evolution of the MoO_3 (010) Surface during Reduction and Oxidation Reactions. Ph.D. Thesis, Carnegie Mellon University, Pittsburgh, PA, 1998.

Table 1. Thicknesses for Films with and without the Presence of Nanodroplets[a]

	$T = 780$ °C		$T = 700$ °C	
	no. of films	mean ± STD (nm)	no. of films	mean ± STD (nm)
without nanodroplets	97	1.54 ± 0.30	34	1.30 ± 0.31
with nanodroplets	6	1.85 ± 0.34	2	1.90 ± 0.14
level of significance (1−α)	99.3%		99.5%	

[a] Levels of significance (1−α), calculated using a statistical *t* test, represent the confidence that the two groups of data represent distinct populations.[29]

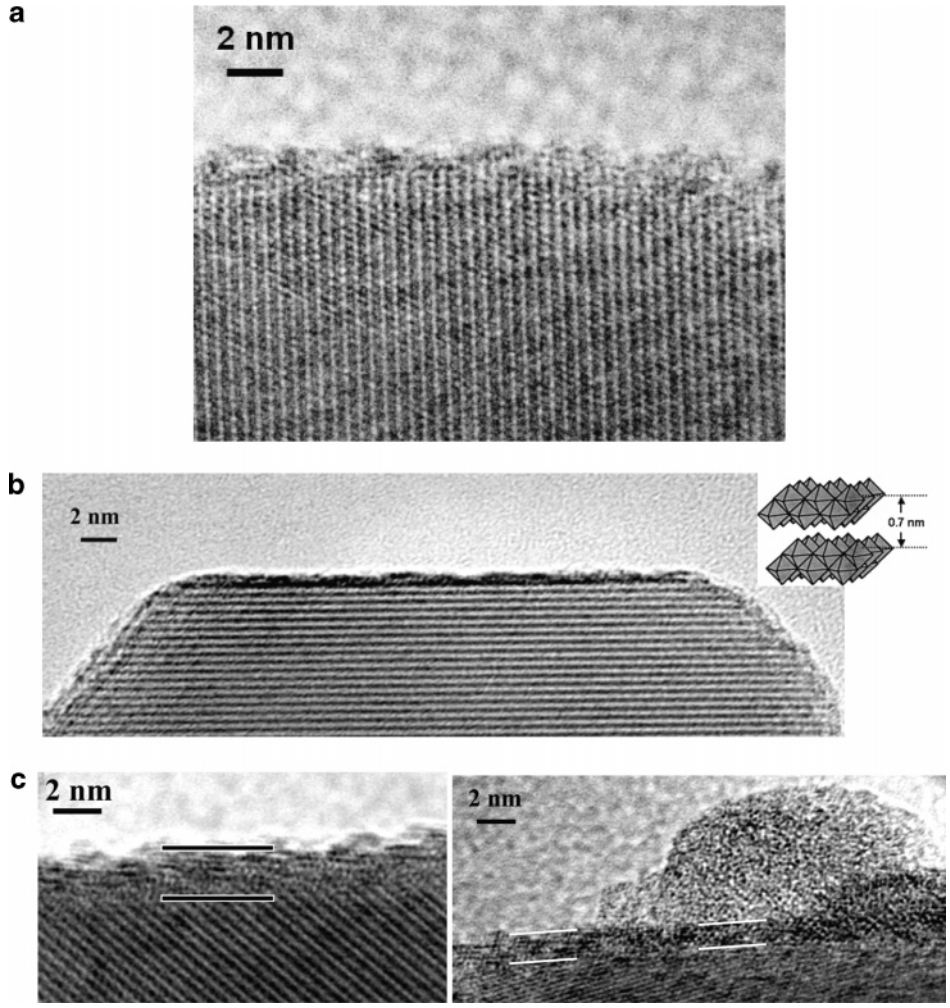

Figure 7. (a) Dry surface with Mo segregation within or on the Al_2O_3 crystal structure observed in a lower temperature range (450−650 °C) exemplified by an Al_2O_3 + 9% MoO_3 sample equilibrated at 450 °C. (b) Double-octahedral adsorbed layer of MoO_3 or one layer of the α-MoO_3 structure[30] as shown in the inset, as formed on a large fraction of surfaces at relatively higher temperature (900−1000 °C). (c) Disordered surficial films (1−2 nm thick) observed only on a small fraction of surfaces. Such films were sometimes also observed to coexist with nonwetting droplets. This MoO_3-saturated sample was equilibrated at 975 °C.

(4) a composition highly enriched in the end member that comprises the adjacent crystal, as compared with the equilibrium bulk liquid.

The Bi_2O_3-enriched surficial films preferentially form on ZnO $\{11\bar{2}0\}$ surfaces, whereas $\{1\bar{1}00\}$ facets are devoid of films.[17] The $\{11\bar{2}0\}$ surface of ZnO has an epitaxial relation with the δ-Bi_2O_3 {100} facet,[17] which not only stabilizes the SAF by lowering the interfacial energy but also imposes significant order in the adjacent Bi_2O_3-enriched films. The SAFs exhibit a lateral partial order (Figure 3b) whose period is double the ZnO $\{1\bar{1}00\}$ lattice spacing (0.281 nm) and roughly equal to the lattice constant of cubic δ-Bi_2O_3 (0.565 nm), supporting the induced-order hypothesis. However, these films are not simply epitaxial layers of the δ-Bi_2O_3 phase because the interlayer distance (∼0.4 nm) is intermediate to the lattice distances of the δ-Bi_2O_3 {100} (0.565 nm) and the ZnO $\{11\bar{2}0\}$ (0.325); in addition, the films contain only ∼18 mol % Bi_2O_3.[17] The partial order observed in HRTEM often depends on the alignment of crystalline orientation and other imaging conditions. Some order likely intensifies during the quench.

The surficial films in ZnO−Bi_2O_3 clearly exhibit equilibrium thicknesses and disappear below a transition temperature. The temperature-dependent film thickness is clearly reversible for Bi_2O_3-saturated samples; the true equilibrium values are likely bounded by the measured mean thicknesses for the two types of samples that initially have no films or thicker films (Figure 4). A similar temperature-dependent trend was observed for MoO_3 on Al_2O_3, where high levels of adsorption were observed at higher temperatures, though the majority of adsorbates appear to be ordered bilayers (Figure 7b). The formation of partially ordered surficial films containing adsorbates

at thermal equilibrium should be consistent with the Gibbs adsorption theory. The Gibbs isotherm should apply, specifying the relation between surface energy and surface excess; in this regard, the excess energy of the entire SAF represents the excess free energy γ_{cv} for the ZnO surface. However, this thermodynamic relation alone cannot predict actual film characteristics, such as thickness or composition.

The appearance of atomically abrupt film−crystal interfaces and rather discrete films as shown in Figures 1−3 would support a simplified treatment of the film free energy in the pressure-balance model extended from the original Clarke model for intergranular films.[1,4,10,12−13] In such an approach, the excess free energy associated with the surficial film as a function of film thickness h is written as

$$G^x(h) = (\gamma_{cl} + \gamma_{lv}) - \frac{A_{123}}{12\pi h^2} + |\Delta\gamma| e^{-h/\xi} + (\Delta G_{vol} h) \quad (1)$$

The first term in eq 1 is the sum of the excess free energies for a crystal−liquid interface and a liquid−vapor interface. These are well-defined thermodynamic quantities, and the following equation should be held rigorously for a thick liquid film of equilibrium composition with a well-separated surface and interface:

$$G^x(h = +\infty) = \gamma_{cl} + \gamma_{lv} \quad (2)$$

The second term in eq 1 is the nonretarded London dispersion interaction. For the Bi_2O_3−ZnO eutectic liquid on ZnO, the dispersion interaction is attractive, and Hamaker constant A_{123} for the system air(1)/film(2)/substrate(3) was calculated from measured optical properties to be +137 zJ.[17] The third term is a repulsive interaction approximated by a generic exponentially decaying form,[13,27] which may represent structural,[1,16] chemical,[12] and electrostatic[4] contributions where $|\Delta\gamma|$ is the differential interfacial energy between surfaces with no film and an infinitely thick film (excluding the contribution from the dispersion interaction) and ξ is a characteristic coherence length. Finally, ΔG_{vol} is the volumetric Gibbs free energy for forming a uniform liquid (or glassy) film of the average composition from a reservoir of equilibrium bulk phases. This term is zero for a wetting liquid film of the same composition as the bulk equilibrium liquid but becomes significant in magnitude below the bulk eutectic temperature where the bulk liquid or glass is metastable or when the film has an average composition distinct from that of the equilibrium bulk liquid.

In this pressure-balance model, the equilibrium thickness corresponds to a minimum excess free energy. Because the spatial derivatives of the interactions in eq 1 are equivalent to pressures acting across the film, the equilibrium thickness is alternatively specified by a balance of two attractive pressures and one repulsive pressure:

$$\frac{A_{123}}{6\pi h^3} + \Delta G_{vol} = \frac{|\Delta\gamma|}{\xi} e^{-h/\xi} \quad (3)$$

This rather simplified model can elucidate the general trends observed in Figure 4. Below the bulk eutectic temperatures, the volumetric amorphization energy is likely to overwhelm the dispersion pressure.[17] Consequently, with decreasing temperature, the increasing attractive pressure associated with the effective volume term ΔG_{vol} reduces the film thickness and likely leads to a drying transition well below the eutectic wherein the surficial film virtually vanishes (but submonolayer adsorption may still persist). With increasing temperature, perfect wetting is expected to be delayed above the eutectic temperature in the presence of an attractive dispersion pressure, or any other attractive interaction, such as the strain energy due to partial epitaxy. The latter is not yet considered in this model.

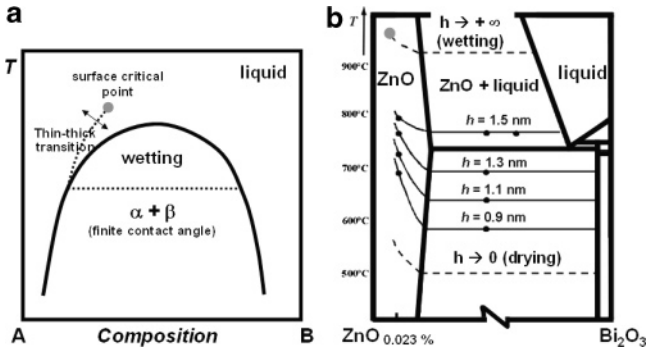

Figure 8. (a) Schematic illustration of Cahn's prewetting model.[20] (b) Surficial films observed in this study may be interpreted as a case of prewetting in a two-component oxide system with a deep eutectic reaction. Lines of constant thickness, corresponding to constant adsorption, are plotted in the phase fields of the ZnO−Bi_2O_3 binary phase diagram. Actual temperature-dependent film thicknesses were interpolated from HRTEM measurements to give the approximate thickness contours shown in the phase diagram. Subsolidus data (single-phase field) are from ref 17.

An attempt to refine this model would require knowing the actual compositions of the SAFs, which reveals a fundamental limitation of the pressure-balance model based on a homogeneous film composition. The composition should derive from a compromise. Specifically, to minimize the volume penalty, the composition should be close to that of the bulk liquid; to minimize the interfacial transition energy, it should be closer that of the bulk substrate; and to minimize the surface transition energy, it should be closer that of a region near the surface of the bulk liquid. Obviously, this can be better achieved by having through thickness gradients in the surface film, but then further energy penalties exist that can be explicitly described in the context of diffuse interface theories.

Thus, the sequence of adsorption and wetting events in Bi_2O_3 on ZnO $\{11\bar{2}0\}$ facets as a function of temperature and composition may be alternatively and better interpreted as a case of prewetting, as a generalization of that proposed by Cahn for binary immiscible liquids[20−22] and confirmed for organic and metallic liquids[23−26] (a schematic phase diagram of which is depicted in Figure 8a). For comparison, lines of constant SAF thickness, resembling the constant adsorption or Gibbs surface excess lines, are plotted in the ZnO−Bi_2O_3 binary phase diagram in Figure 8b. The film thickness exhibits a temperature dependence counter to that expected from the adsorption level in a Langmuir−McLean model[31] but is consistent with that of the prewetting model, decreasing monotonically with decreasing temperature in the range below the eutectic at 740 °C until nearly vanishing at a surface drying temperature between 450 and 600 °C. A Langmuir-type submonolayer adsorption may occur below the drying temperature but is not described by the Cahn model. With increasing temperature, the Bi_2O_3-rich films persist well

(31) Dash, J. G. In *Films on Solid Surfaces: The Physics and Chemistry of Physical Adsorption*; Academic Press: New York, 1975.

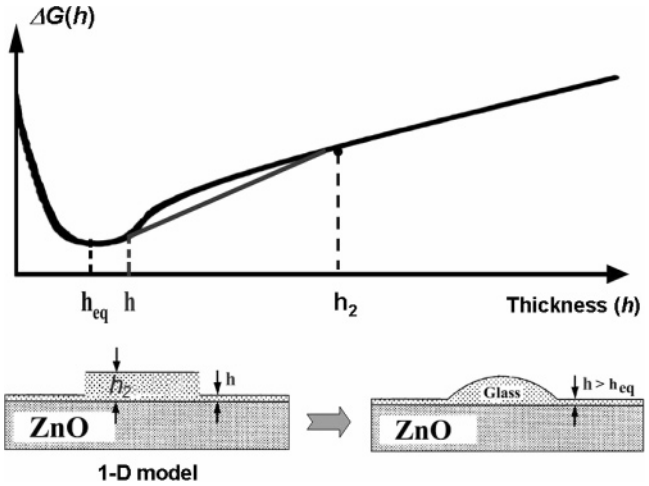

Figure 9. Sketch of the free-energy curve versus film thickness, in which it is shown that for films sufficiently thicker than the equilibrium value the energy can be reduced by spontaneous separation into thicker and thinner regions. This indicates the condition for which nanodroplets can form spontaneously but only with wavelengths long enough that curvature forces are not inhibiting.

into the solid−liquid coexistence regime. However, perfect wetting of the Bi_2O_3-enriched liquid was previously reported on the polycrystalline ZnO surface at ~920 °C.[32] Perfect wetting also occurs at grain boundaries in Bi_2O_3-doped ZnO at ~950 °C.[33] Thus, perfect wetting may reasonably be expected to occur on the {11$\bar{2}$0} surface above 900 °C. This situation is more complex than the associated thin−thick transition and surface critical point expected in the single-phase region above the wetting temperature for the Cahn model. In the present case, there are two transitions—one for the onset of thick adsorption layers and a second for the transition to complete wetting (meaning $\theta = 0$ in Figure 6 and $\gamma_{sv} = \gamma_{sl} + \gamma_{lv}$) above which surface films are arbitrarily thick, where here the latter occurs at a distinctly higher temperature, as depicted in Figure 4.

It is of interest to consider further the origin and effects of the nanodroplets. If a film is thicker than the equilibrium level, then there is a driving force to transport the extra adsorbate to any bulk second phase. If a film is sufficiently thick, then it is unstable to spontaneous breakup into thinner regions and incipient droplets, as is depicted in Figure 9. This may have occurred occasionally in some films that were initially much thicker and had not fully equilibrated. However, we note that in the small droplet the curvature will lead to an internal pressure, P, of order $\kappa\gamma_{lv}$, where κ is the curvature. If $\kappa = {}^2/_R \approx {}^1/_5$ nm and if $\gamma_{lv} \approx 0.2$ J/m^2, then $P \approx 40$ MPa for droplets such as that in Figure 6. This should be balanced by disjoining and attractive forces of similar magnitude in the nearby SAF, but with a lateral gradient to drive the diffusion or viscous flow leading to the formation and coarsening of the nanodroplets. This pressure level is much higher than the computed attractive dispersion forces (~1−5 MPa).[17] This may imply that the films at and above the eutectic temperature experience an order of magnitude higher, unaccounted for attractive force than that computed from the dispersion forces[17] balanced by a higher, unaccounted for disjoining force. This could also then imply that a much larger difference in composition exists between the SAF and the liquid and a higher associated ΔG_{vol} exists for SAFs[17] above the eutectic temperature than that which follows from assuming that only a dispersion force resists complete wetting.

In two binary oxide systems, we have observed the formation of nanometer-thick SAFs on crystal surfaces, with evidence of partial order and which exist within a wide range of temperature, bounded by two different transitions, with the latter being well above the eutectic temperature. We refer to these as drying and complete wetting transitions, and the intervening region of equilibrium films corresponds to moist surfaces. Somewhat similar regions of multilayer disordered films existing for a range of chemical potentials between those giving thinner surface coverage and perfect wetting have been observed in organic or aqueous fluid−fluid systems elsewhere and have been described as frustrated complete wetting.[34] A similar condition of a finite droplet (with $\theta > 0$) surrounded by a finite pure liquid film with thickness limited by dispersion forces has been referred to as pseudopartial wetting.[35] Pseudopartial wetting has also been observed for immiscible metal systems such as Bi−Pb alloys on the Cu (111) surface,[36−38] wherein a droplet with a finite contact angle coexists with submonolayer adsorbates (termed precursor films in refs 36−38), indicating the widespread existence of parallel phenomena in systems of different materials. Below this drying transition, the oxide surfaces may also experience Langmuir-like, submonolayer adsorption. Such has been seen in the MoO_3−Al_2O_3 system. In the Bi_2O_3−ZnO system, the situation is more complicated because the {11$\bar{2}$0} surface is not thought to be stable for pure ZnO and so is not readily available for study. However, the occasional existence of dry surfaces with this orientation suggests that they are stabilized to some degree by Bi_2O_3 adsorption. Above the wetting condition, $\theta = 0$ and $\gamma_{sv} = \gamma_{sl} + \gamma_{lv}$, and the films would be arbitrarily thick. Such films have not been seen on this ZnO {11$\bar{2}$0} surface, but such a wetting transition has been reported for a polycrystalline sample[33] and can be expected for this surface at some temperature between 780 and 950 °C. We reserve the term wetting only for arbitrarily thick layers and do not identify situations in which one might have expected wetting but for dispersion forces, as discussed elsewhere,[34−35] because what prevents complete wetting is yet unclear in these oxide systems. What is clear from Figure 6 is that bulk liquid does not wet the multilayer-covered surface.

5. Conclusions

Experimental observations have been made of the structure, the reversible temperature dependence of the film thickness, and drying (complete dewetting) of surficial films for ZnO−Bi_2O_3. In quenched samples, Bi_2O_3-enriched films exist on ZnO {11$\bar{2}$0} and exhibit some degree of partial order consistent with induced order at the film−substrate interface. With decreasing temperature, the disordered films in Bi_2O_3-doped ZnO persist below the bulk eutectic temperatures with gradual thinning upon cooling until drying occurs at a lower transition temperature. Although less completely characterized, surface films of MoO_3 on Al_2O_3 showed qualitatively similar

(32) Li, J.-G. *J. Mater. Sci. Eng. Lett.* **1994**, *13*, 400−403.
(33) Lee, J.-R.; Chiang, Y.-M. Unpublished work.

(34) Bertrand, E.; Dobbs, H.; Broseta, D.; Indekeu, J.; Bonn, D.; Meunier, J. *Phys. Rev. Lett.* **2000**, *85*, 1282−1285
(35) Brochard-Wyart, F.; di Meglio, J.-M.; Quéré, D.; de Gennes, P. G. *Langmuir* **1991**, *7*, 335−338.
(36) Moon, J.; Lowekamp, J.; Wynblatt, P.; Garoff, S.; Suter, R. M. *Surf. Sci.* **2001**, *488*, 73−82.
(37) Moon, J.; Yoon, J.; Wynblatt, P.; Garoff, S.; Suter, R. M. *Comput. Mater. Sci.* **2002**, *25*, 503−509.
(38) Moon, J.; Garoff, S.; Wynblatt, P.; Suter, R. *Langmuir* **2004**, *20*, 402−408.

behavior. The sequence of adsorption and wetting events in these systems can be interpreted as a case of prewetting, with a perfect-wetting transition being expected at higher temperature. Observations of a second class of thicker films coexisting with nanodroplets illustrate that the liquid does not wet the disordered surface layer.

Acknowledgment. This work was supported by the U.S. Department of Energy, Office of Basic Energy Sciences, DMSE under grant no. DE-FG02-87ER45307 (for Y.-M.C. and J.L.) and under contract no. DE-AC03-76SF00098 (for R.M.C.). J.L. also acknowledges partial support from Clemson University, and Y.M.C., from an NSF/EU NANOAM collaboration (NSF DMR-0010062 and EUG5RD-CT-2001-00586). We are indebted to Professor W. C. Carter, Dr. C. M. Bishop, and M. Tang for critical discussions.

LA0505420